2021-08-01

Interaction Of Kinesin-5 Motor Domain With Tubulin Dimer

Chitra B. Karki
University of Texas at El Paso

INTERACTION OF KINESIN-5 MOTOR DOMAIN WITH TUBULIN DIMER

CHITRA BAHADUR KARKI

Master's Program in Computational Science

APPROVED:

Lin Li, Ph.D., Chair

Jainjun Sun, Ph.D.

Jorge A. Munoz, Ph.D.

Stephen L. Crites, Jr., Ph.D.
Dean of the Graduate School

INTERACTION OF KINESIN-5 MOTOR DOMAIN WITH TUBULIN DIMER

by

CHITRA BAHADUR KARKI, M.S.

THESIS

Presented to the Faculty of the Graduate School of

The University of Texas at El Paso

in Partial Fulfillment

of the Requirements

for the Degree of

MASTER OF SCIENCE

Department of Computational Science

THE UNIVERSITY OF TEXAS AT EL PASO

August 2021

Abstract

Kinesin-5 in fission yeast also known as Cut7 is a molecular motor essential for separation of spindle fibers during the mitotic cell division. Kinesin-5 crosslinks the spindle microtubules and slides them towards the spindle poles. Molecular dynamics simulation was performed, and various analysis were carried out to study the interaction of kinesin-5 motor domain with alpha and beta tubulins. From electrostatic potential distribution, it is observed that binding interface of kinesin-5 motor domain is mainly positive and tubulin dimer is mainly negative, which shows the stronger interaction between them. Further when electric field lines were plotted, we observed more field lines at kinesin-5 motor and beta tubulin interface. Meaning the interaction of kinesin-5 with beta tubulin is stronger. Moreover, the binding energies, salt-bridges, hydrogen bonds, were analyzed in detail, which again supported the stronger interaction of kinesin-5 motor with beta tubulin. Furthermore, key residues at the binding interfaces of kinesin-5 motor domain and tubulin dimers were identified, which are believed to be useful for developing drug against cancerous cells.

Table of Contents

List of Tables

List of Figures

Chapter 1: Interaction of Kinesin-5 Motor Domain with Tubulin Dimer.

1.1 INTRODUCTION

Kinesin-5 is the molecular motors which play essential role in separation of spindle fibers during mitotic cell division [1]. It utilizes ATP to generate force to slide the antiparallel spindle microtubules [2, 3]. The kinesin-5 motor protein is a homo-tetrameric assembly crosslinked by two dimeric subunits folded in antiparallel arrangement [4-7]. The failure of kinesin-5 causes the catastrophic failure of mitosis cell division [8-13]. Which may cause problem in sustaining life as cell division is the fundamental for producing new lives or can bring abnormalities like cancers. In this study, we basically investigated the interaction of kinsin-5 motor domain of fission yeast also known as Cut7 [14] to the tubulin dimer, i.e., alpha and beta. First the molecular dynamic simulation was performed using NAMD [15] for 50 ns. And various multi-scale analyses were performed to study the interaction between kinesin-5 motor domain and tubulin dimer. From electrostatic potential distribution, we observed that the binding interfaces of kinesin-5 motor domain and tubulin dimer are oppositely charged. Which shows there is strong interaction. Further, when electric field lines were plotted, we observer the denser electric field lines passing through the kinsin-5 motor domain and beta tubulin interface. Which indicates the interaction of kinesin-5 motor domain is stronger relative to its interaction with alpha tubulin. The binding energy calculation and salt bridges analysis also advocated the stronger interaction of kinesin-5 motor domain with beta tubulin. This may hint that when kinesin-5 motor domain detaches from microtubule, it first detaches for alpha tubulin. But we don't have the direct evidence. From salt bridges analysis at the interfaces of kinesin-5 motor domain and tubulin dimer, key residues were predicted. This could be valuable information for the drug development against the cancerous cells.

In summary, we observed that there is favorable binding of kinesin-5 motor domain with tubulin dimer from electrostatic point of view, during the process of complexation. Detailed study showed the strong interaction of kinesin-5 motor domain with beta tubulin. This may suggest that when kinesin-5 motor domain detaches from microtubule to take a step, it detaches from alpha tubulin first. Further, the binding energy calculation and salt bridges analysis also advocated the strong interaction of kinesin-5 motor domain with beta tubulin. From salt bridges analysis key residues were identified at the binding interfaces. These residues could be the important targets for the development of anti-cancerous drugs.

1.2 METHODS

1.2.1 Getting Structure and Modeling Missing Loop

The 3D coordinates of cut-7 motor domain and the tubulin dimer was downloaded from RCSB Protein Data Bank [14]. The missing loop of motor domain near C-terminal (Figure 1.1 a) was modeled with SWISS-MODEL [16]. The modeled structured was then subjected to molecular dynamics simulation (Figure 1.1 b).

1.2.2 Molecular Dynamics Simulation

The molecular dynamics simulation was performed using program NAMD [15]. A cubic box of TIP3 [17] water of thickness 10 Å from the protein was used to solvate the simulating system. Na^+ and Cl^- ions were used to neutralize the system first and was later maintained in 0.15 mol/liter of NaCl concentration to mimic the native environment. Solvation and ionization of the simulating system was performed with VMD [18]. Periodic boundary condition was applied on the solvation box and PME [19, 20] was use for the long-range electrostatic interaction beyond 12 Å. Charmm-36 force field [21] was used for parametrization of protein, water, and ions. The temperature and the pressure were set to 300 K and 1 atm, respectively. The system was then

simulated with program NAMD with 20,000 steps of minimization followed by 50 ns of equilibration.

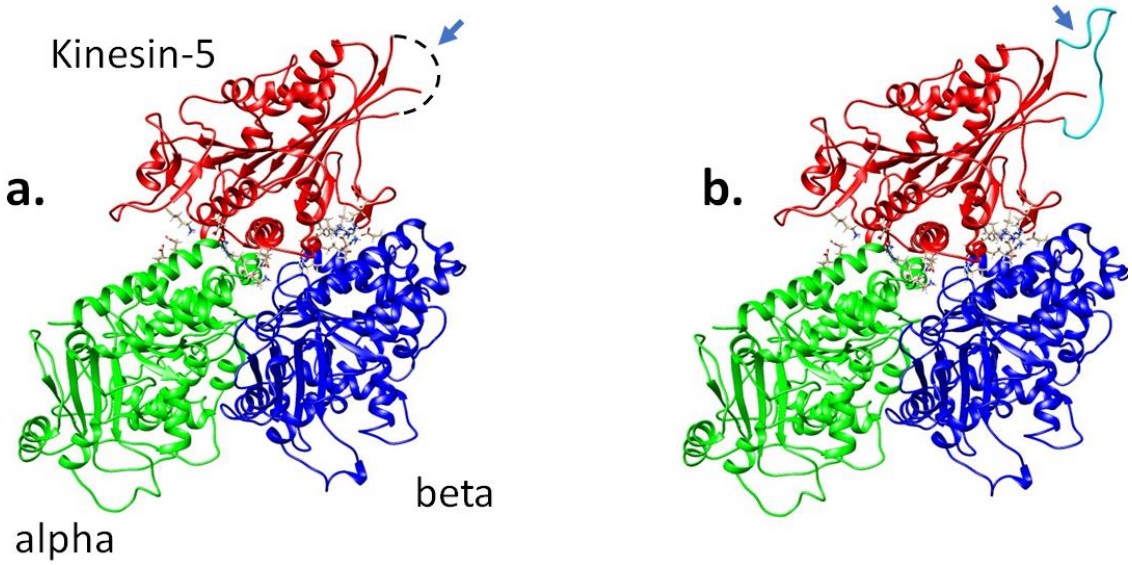

Figure 1.1: Modeling the missing loop and the simulation structure. (a) Structure obtained from form Protein Data Bank (PDB ID: 5MLV). Out of six such trimers, one was isolated for the simulation. The missing portion near the C-terminal of kinesin-5 motor domain is represented as dotted line and pointed with arrow. Kinesin-5 motor domain, alpha and beta tubulins are represented in red, green, and blue, respectively. (b) The missing portion was modeled with SWISS-MODEL. Which is represented by cyan color and pointed with arrow.

1.2.3 Root Mean Square Deviation (RMSD)

The root mean square deviation (RMSD) was evaluated in VMD for the heavy atoms (without hydrogen atoms) with respect to the initial configuration of the structure for the purpose of stability check, Figure 1.2.

1.2.4 Binding Energy Calculation

To estimation the binding affinity between kinesin motor and tubulins (alpha and beta), the MM/PBSA (molecular mechanics/Poisson Boltzmann surface area) method [22] was used as in our previous works [23, 24]. The 500 sample structures in a step of 0.1 ns were extracted from 50 ns NAMD simulation for the MM/PBSA analysis. And the total binding affinity is given as,

$$\Delta E = < \Delta E_{coul} > + < \Delta E_{vwd} > + < \Delta E_{pol} > + < \Delta E_{np} >$$

The Coulombic energy (E_{coul}) and Polar solvation energy (E_{pol}) were calculated with DelPhi program [25-27]. The charges and radii of the atoms were assigned by PDB2PQR [28] program. The dielectric constants for protein and water were set to 2 and 80, respectively. Similarly, the resolution was set to 2 grids/Å, salt concentration to 0.15 mM and probe radius to 1.4 Å. The 70 % of DelPhi calculation box was set to covered by protein. The Van der Waals energy (E_{vwd}) was calculated with NAMD, subjecting the sample structures to one step of equilibration. For the non-polar solvation energy (E_{np}), solvent accessible surface area (SASA) was calculated with program NACCESS (ref) using water as probe with radius 1.4 Å and converted to energy with the relation,

$$E_{np} = \alpha \cdot SASA + \beta$$

$\alpha = 0.0054$ and $\beta = 0.92$ kcal/mol

For kinesin and beta interface, the energy terms: ΔE_{coul} , ΔE_{vwd}, ΔE_{pol} and ΔE_{np} were calculated as below and same strategy was used for kinesin and alpha interface.

$$\Delta E_{coul} = E_{coul(kinesin \cdot beta)} - [E_{coul(kinesin)} + E_{coul(beta)}]$$

$$\Delta E_{vwd} = E_{vwd(kinesin \cdot beta)} - [E_{vwd(kinesin)} + E_{vwd(beta)}]$$

$$\Delta E_{pol} = E_{pol(kinesin \cdot beta)} - [E_{pol(kinesin)} + E_{pol(beta)}]$$

$$\Delta E_{np} = E_{np(kinesin \cdot beta)} - [E_{np(kinesin)} + E_{np(beta)}]$$

1.2.5 Salt Bridge Analysis

Salt bridge analysis at the binding interfaces of kinesin-5 motor domain with the tubulins was performed in VMD based on the same samples collected for MM/PBSA analysis. The cutoff distance between Nitrogen and Oxygen of oppositely charged residues was set to 4 Å. The occupancy of the salt bridges, their binding energies, and mean distances between the residues of salt bridges were also calculated, Table 1.2. Salt bridges with occupancy <10 % were ignored.

The Coulombic and Van der Waals energies were considered for the salt bridges energy calculations. These energies were calculated using NAMD subjected to 1 step of equilibration. The same sample structures, used in binding energy calculation, were utilized to calculate the salt bridge energies.

1.3 RESULTS AND DISCUSSIONS

1.3.1 Stability of the Simulation

From the RMSD analysis (Figure 1.2), it is observed that the RMSD of the simulating system (Figure 1.1) is stable after 10 ns. The RMSD of alpha and beta tubulins are stable almost from the beginning of the simulation whereas the kinesin has little wiggly but stable RMSD after 10 ns. The microtubule is the assembly of the tubulins, which is like a highway in the cytoskeleton of cells, upon which kinesin motors can walk through with hand-on-hand mechanism. Hence, the kinesin motor undergoes lot of mechanical stress and conformational changes. This could be the reason why the kinesin motor has higher and wiggly RMSD relative to tubulins.

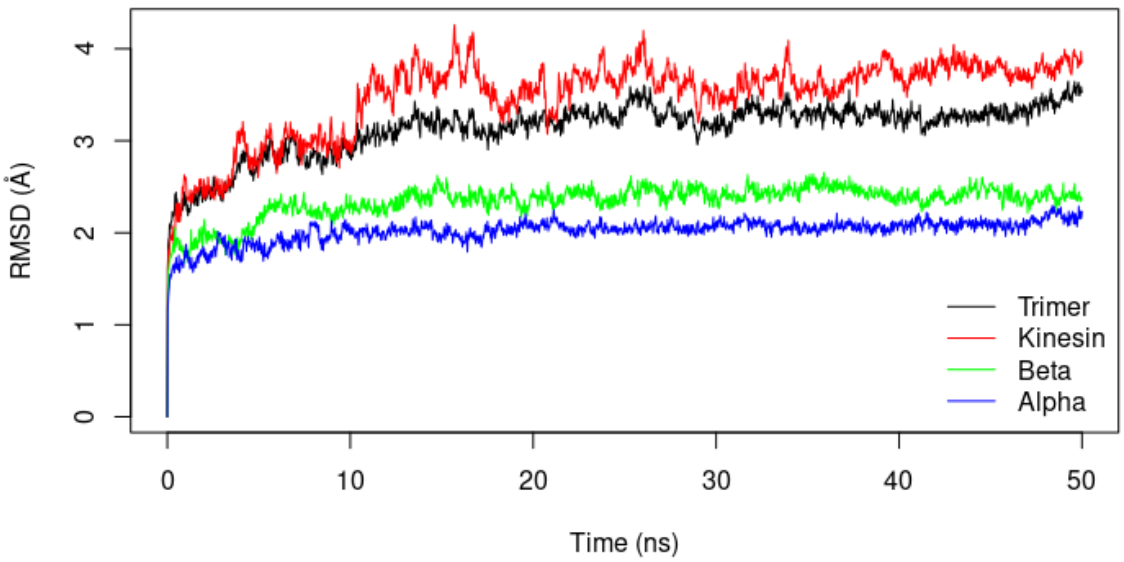

Figure 1.2: Root mean square deviation (RMSD) analysis of the system. Trimer represents the complex of kinesin-5 motor domain interacting with alpha and beta tubulins. The system becomes stable almost after 10 ns.

1.3.2 Strong Binding Affinity of Kinesin-5 Motor with Beta Tubulin

The binding energy calculation (Table 1.1) shows the average binding energies of kinesin/beta complex and kinesin/alpha are -80.55 kcal/mol and -70.42 kcal/mol, respectively. This reflects the binding strength of kinesin-5 motor domain to beta tubulin is stronger than kinesin-5 motor domain to alpha tubulin by approximately 10 kcal/mol. In both complexes, Van der Waals energy (ΔE_{vwd}) and non-polar solvation energy (ΔE_{np}) contribute significantly to the total average binding energy (ΔE). Although the attractive Coulombic energy (ΔE_{coul}) is much higher in comparison to the other energies in both complexes, it is compensated by the dehydration of the polar and charged residues (polar solvation energy (ΔE_{pol})) at the binding interfaces when kinesin binds with tubulin dimer.

Table 1.1: Binding energy calculation from MM/PBSA analysis. SD represents standard deviation. The angle bracket (< >) means the average. For example, $<E_{vwd}>$ is Van der Waals energy averaged by the total number of sample frames.

Energy terms	Energy (kcal/mol)			
	motor/beta	SD*	motor/alpha	SD
$<E_{vwd}>$	-52.22	8.99	-62.55	7.63
$<E_{coul}>$	-499.37	40.82	-153.34	31.80
$<E_{pol}>$	483.60	39.66	158.18	28.42
$<E_{np}>$	-12.56	1.04	-12.70	0.72
ΔE	-80.55		-70.42	

SD*; standard deviation

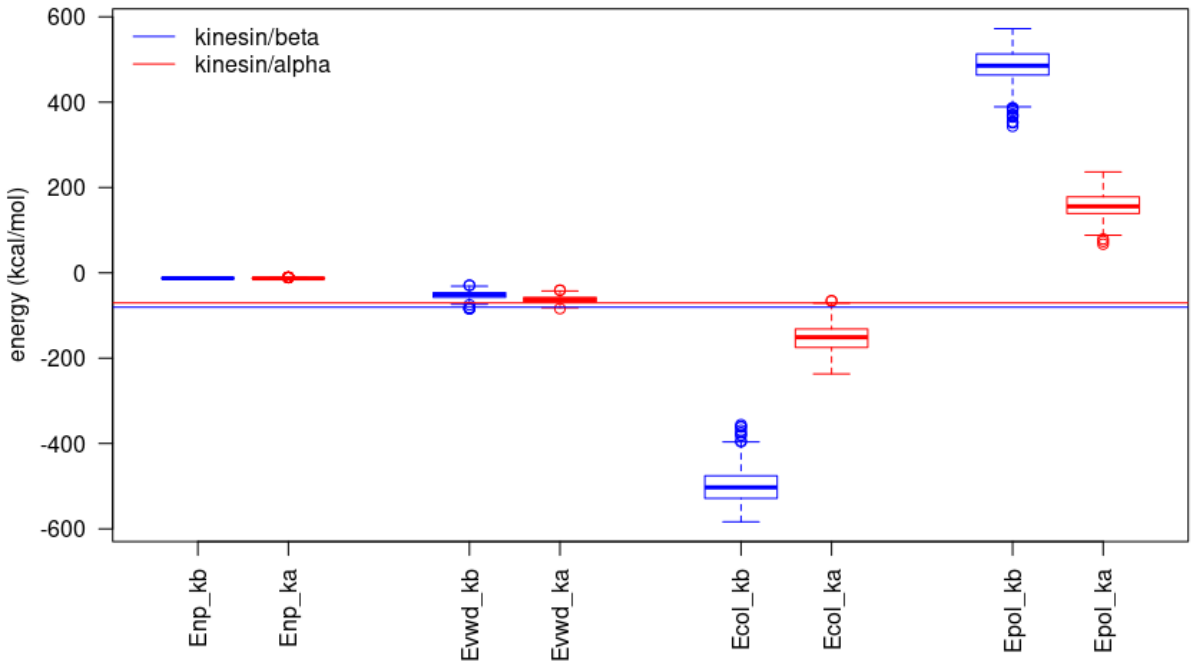

Figure 1.3: Distribution of the different energy terms associated in MM/PBSA analysis. Color blue indicates the kinesin/beta complex while red indicates the kinesin/alpha complex. The blue and red horizontal lines are average binding energies of kinesin/beta and kinesin/alpha, respectively i.e., -80.55 kcal/mol and -70.43 kcal/mol (see Table 1).Root mean square deviation (RMSD) analysis of the system. Trimer represents the complex of kinesin-5 motor domain interacting with alpha and beta tubulins. The system becomes stable almost after 10 ns.

1.3.3 Electrostatically Favorable for Binding of Kinesin-5 Motor with Tubulins

For the protein-protein or protein-ligand interaction electrostatic plays vital role. To investigate the further details about the interaction of kinesin motor domain with alpha and beta tubulins from electrostatic point of view, electrostatic potential distribution over the surface of kinesin motor domain and tubulins were mapped, Figure 1.4 (b, c, d). The binding interface of the kinesin-5 motor domain is mostly positive, Figure 1.4 (b). Similarly, the binding interfaces of alpha and beta to kinesin-5 motor domain are mostly negative, Figure 1.4 (c). Which means there will be a strong interaction of kinesin-5 motor domain with alpha and beta tubulins when it binds to the tubulin dimer. The strong interaction of kinesin motor domain with tubulins may help its

counterpart to successfully take a step to the correct future binding position on the same microfilament by sticking firmly in its place because two kinesin motor domains are interlinked with neck linker and coiled coil stalk.

When we further dig in details of the electrostatic interaction, it is observed that the density of electric field lines passing through kinesin-5 motor domain and beta tubulin interface is greater than kinesin-5 motor domain and alpha tubulin interface, Figure 1.4 (d). This illustrates the interaction of kinesin-5 motor domain is stronger with beta tubulin. It is consistent with binding energy calculation, Table 1.1.

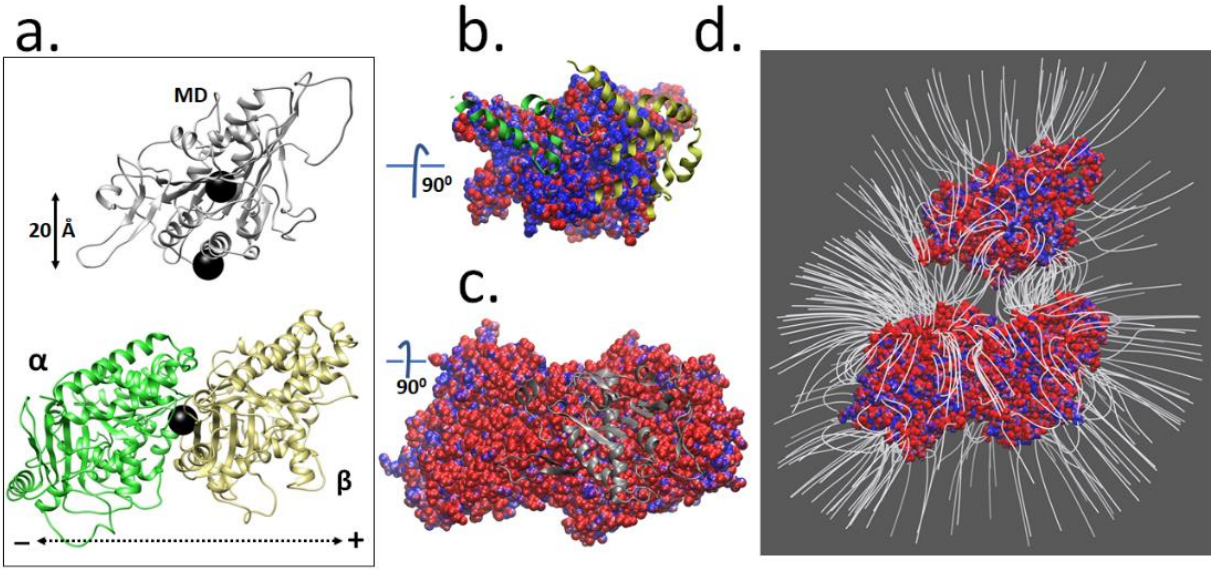

Figure 1.4: Electrostatic potential distribution over the surface and electric field lines. (a) Kinesin motor domain separated by 20 Å from its binding position away for the line joining the center of mass of alpha/beta tubulins and kinesin motor domain. The black spheres from bottom to top represent the center of mass of alpha/beta tubulins, native binding position of kinesin motor head and final position of motor head after separation. Alpha tubulin, beta tubulin, and kinesin motor domain are shown in green, gray, and silver, respectively. (b) 90-degree clockwise rotation of panel (a) inside the plane with electrostatic potential distribution over the surface focusing the binding interface of kinesin motor head with tubulins. Blue and red colors represent positive and negative potential distribution, respectively. Alpha and beta tubulins are partially shown in cartoon representation. (c) 90-degree anticlockwise rotation of panel (a) out of the plane with electrostatic potential distribution over the surface focusing the binding interface of alpha and beta tubulins. Kinesin motor domain is partially shown in silver color. (d) Electric field lines passing through the binding interfaces of kinesin with the tubulins. Panel (d) is in parallel orientation with panel (a)

1.3.4 Salt Bridges shows Strong Interaction of Kinesin-5 Motor and Beta Tubulin

From binding energy calculations and electric field lines distribution at the binding interface of kinesin-5 motor domain with alpha and beta tubulin, it is observed that kinesin-5 motor domain has stronger interaction with beta tubulin. To investigate this at the atomic level we performed salt bridge analysis at the binding interfaces of kinesin-5 motor domain with alpha and beta tubulins. The salt bridges present at both the interfaces are listed in Table 1.2 and their spatial distribution are presented in Figure 1.7. The beta tubulin and kinesin motor domain binding interface has 8 salt bridges, Table 1.1. The occupancies of the salt bridges are based on the sample frames extracted from 50 ns simulation as described in method section. Columbic and Van der Waals energies were considered for salt bridge energies.

The total salt bridges energy at kinesin-5 motor domain and beta tubulin interface is -28.88 kcal/mol. The Residue, GLU 194 of beta tubulin is interacting with two residues, ARG 233 and LYS 377, of kinesin-5 motor domain. Similarly, the residue GLU 410 of beta tubulin is interacting with two residues, ARG 374 and ARG 380 of kinesin-5 motor domain. The most energetic salt bridge is ASP 417 – ARG 241 with energy -7.36 kcal/mol. It has almost 100 % occupancy and mean distance below the cut off. The weakest salt bridge is GLU 158 - LYS 342 with energy -0.34 kcal/mol. It has lower occupancy and the mean distance greater than the cut off compared to other salt bridges.

Table 2.2: Calculation of salt bridge energies their occupancy based on sample frames and mean salt bridge distances. The units of energies are in kcal/mol. The units of mean distances of salt bridges are in Å. Symbols #, " and * represent residues involved in two salt bridges. Number of samples frames is 500. The extraction of sample frames from 50 ns simulation is mentioned in method section. The negative energies mean attractive interactions. Salt bridges having occupancy < 10% are not listed. The spatial distribution of the salt bridges listed in the table are shown in Figure 1.7. The time evolution of the distances between the residues involved in salt bridges are shown in Figure 1.5 (a) and Figure 1.6 (a).

Interface	Salt-bridges	#. of frames	Occupancy (%)	Energy (kcal/mol)	Mean Distance (Å)
	beta motor				
	ARG 156 - GLU 217	309	61.8	-4.13	5.09
	GLU 157 - ARG 229	110	22.0	-2.65	4.24
	GLU 158 - LYS 342	81	16.2	-0.34	7.45
	GLU 194 # - ARG 233	320	64.0	-2.18	4.55
beta/motor	GLU 194 # - LYS 377	474	94.8	-1.63	3.58
	GLU 410 " - ARG 374	338	67.6	-5.54	3.76
	GLU 410 " - ARG 380	473	94.6	-5.00	3.48
	ASP 417 - ARG 241	499	99.8	-7.36	3.37
				-28.88	
	alpha motor				
	LYS 116 - GLU 340	228	57.6	-1.05	5.68
	LYS 405 - GLU 366	395	79.0	-1.63	3.54
alpha/motor	ARG 406 - GLU 413	149	29.8	-3.74	4.36
	GLU 415 - ARG 345	488	97.6	-6.47	3.42
	GLU 418 - ARG 336	499	99.8	-6.12	3.40
	GLU 424 - LYS 118 *	56	11.2	-0.29	5.39
	GLU 427 - LYS 118 *	475	95.8	-2.54	2.98
				-21.84	

#, " , *: represent residues involved in two salt bridges.

The salt bridges energy of kinesin-5 motor domain and alpha tubulin interface is -21.84 kcal/mol. The residue, LYS 118 of kinesin-5 motor domain interacted with two residues, GLU 424 and GLU 427, of alpha tubulin. The salt bridges GLU 415 - ARG 345 and GLU 418 - ARG 336 have almost same energy and are the most energetic salt bridges at kinesin-5 motor domain and alpha tubulin interface. Also, they have higher occupancies, and the mean distances close the cut

off relative to other salt bridges. The salt bridge, GLU 424 - LYS 118 is the weakest at this interface with energy -0.29 kcal/mol. It has lower occupancy and the mean distance above the cut off compared to other salt bridges. Interestingly, the salt bridge GLU 427 - LYS 118, which shares the LYS 118 with GLY 424, is relatively stronger. It is because the salt bridge GLU 427 – LYS 118 has higher occupancy and mean distance below the cut off. From the above discussion, we observed that the stronger salt bridges have higher occupancies and the mean distance below the cut off.

The formation of multiple salt bridges at the same time frame helps to stabilize the protein-protein interaction. Figure 1.5 and Figure 1.6 shows such analysis of occurrence of simultaneous salt bridges with their time evolution. The number of simultaneous salt bridges for kinesin-5 motor domain and beta tubulin ranges from 3 to 8. While for kinesin-5 motor domain and alpha, it ranges from 2 to 6. In the overlap region, 3 to 5 (Figure 1.5 (d) and Figure 1.6 (d)), the kinesin-5 motor domain and alpha tubulin interface has higher number of simultaneous salt bridges. But for 6 simultaneous salt bridges, kinesin-5 motor domain and beta tubulin interface have higher counts of frames having salt bridges. Moreover, kinesin-5 motor domain and alpha tubulin interface lacks 7 and 8 simultaneous salt bridges. Hence, from simultaneous salt bridge analysis, salt bridges energy calculation and electric field lines, we concluded that during complexation the kinesin-5 motor domain interacts strongly with beta tubulin.

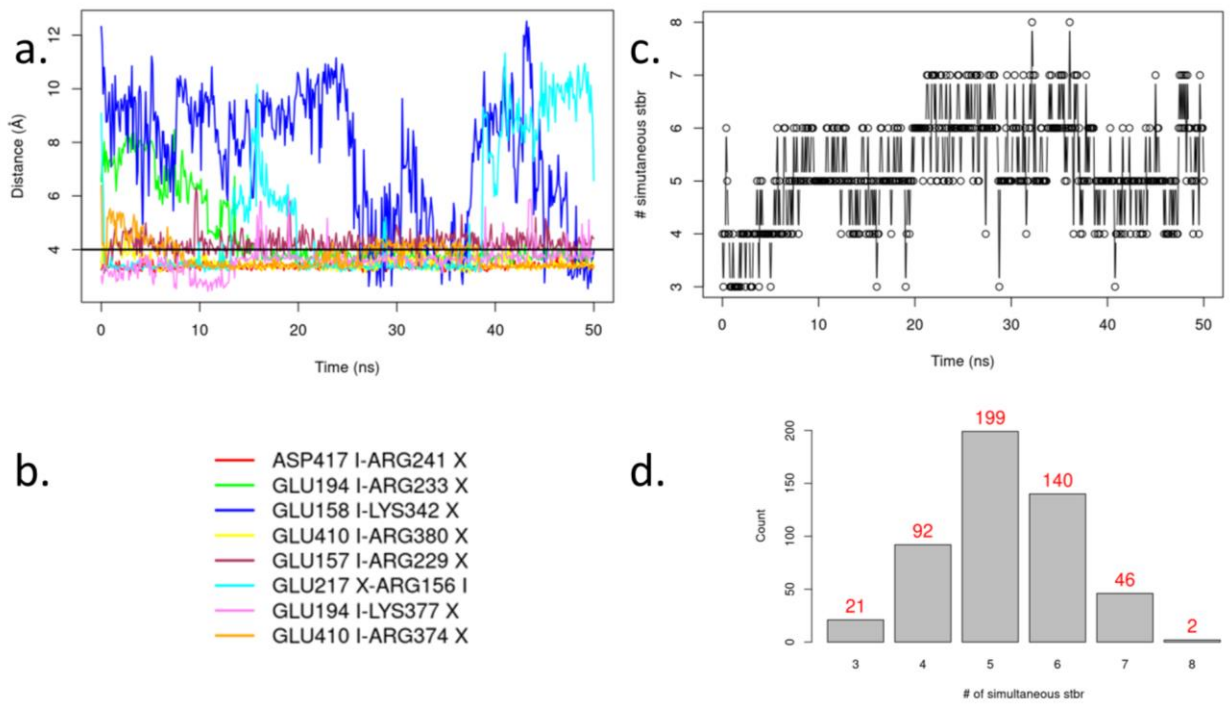

Figure 1.5: Time evolution of salt bridges and their simultaneous occurrence at kinesin-5 motor domain and beta tubulin interface. (a) Time evolution of distances between the residues forming salt bridges at kinesin-5 motor domain and beta tubulin interface. The distances are measured form center of mass of the residues. These residues are listed in Table 1.2. The black horizontal line is the cutoff. Below the line salt bridges are formed and are lost above the line. (b) Legend for the graph in panel (a). X represents kinesin-5 motor domain, and I represents beta tubulin. (c) Time evolution of the simultaneous salt bridges. At kinesin-5 motor domain and beta tubulin interface at most there are 8 simultaneous salt bridges in between 30 and 40 ns for 2 frames. Similarly, at least there are 3 simultaneous salt bridges for 21 frames. These analyses were performed on 500 frames extracted from 50 ns simulation as described in method section.

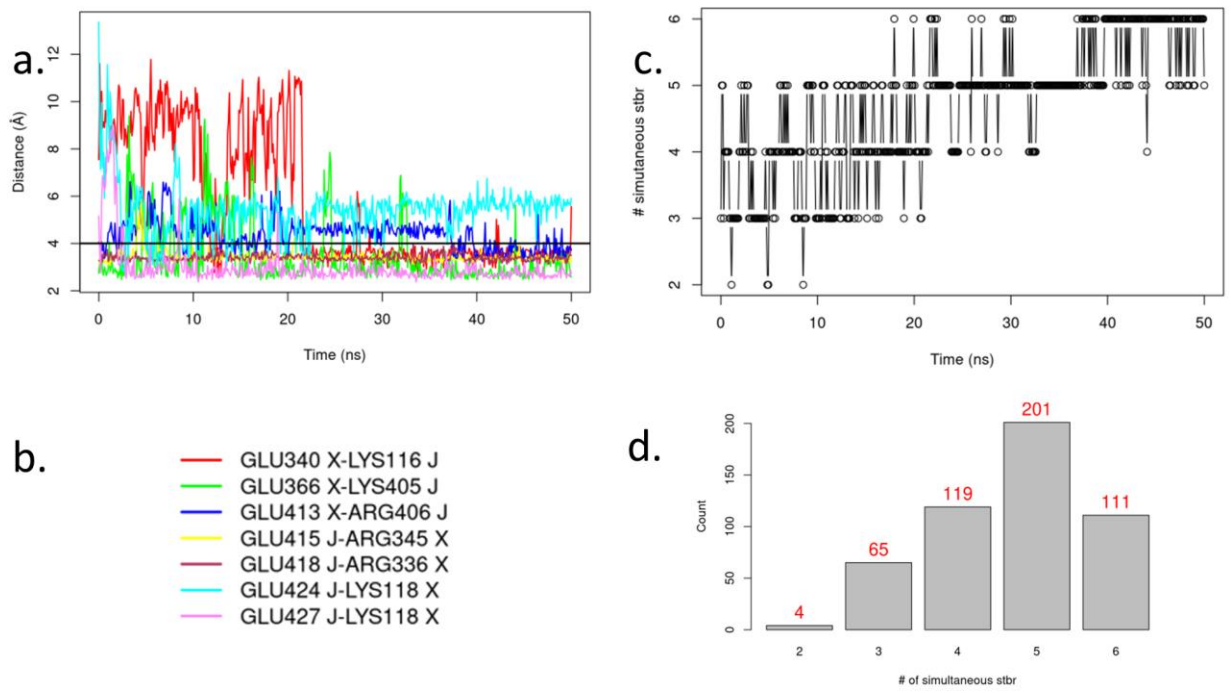

Figure 1.6: Time evolution of salt bridges and their simultaneous occurrence at kinesin-5 motor domain and alpha tubulin interface. (a) Time evolution of distances between the residues forming salt bridges at kinesin-5 motor domain and alpha tubulin interface. The distances are measured from center of mass of the residues. These residues are listed in Table 1.2. The black horizontal line is the cutoff. Below the line salt bridges are formed and are lost above the line. (b) Legend for the graph in panel (a). X represents kinesin-5 motor domain, and J represents alpha tubulin. (c) Time evolution of the simultaneous salt bridges. At kinesin-5 motor domain and beta tubulin interface at most there are 6 simultaneous for 111 frames. Similarly, at least there are 2 simultaneous salt bridges for 4 frames. These analyses were performed on 500 frames extracted from 50 ns simulation as described in method section.

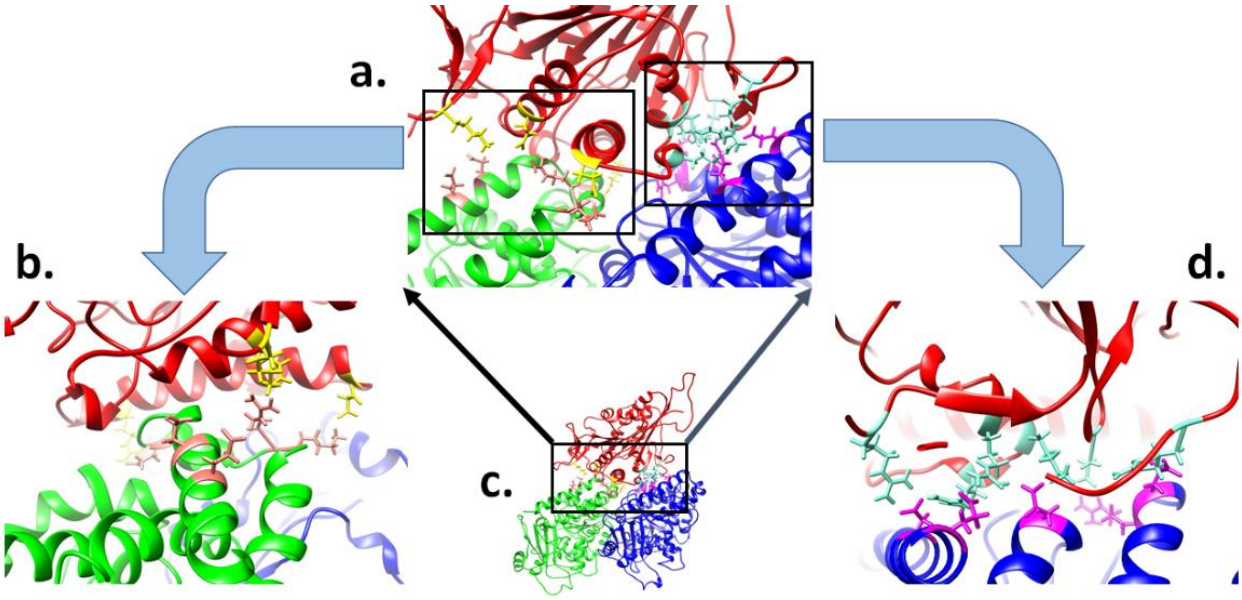

Figure 1.7: Spatial distribution of the salt bridges at the binding interfaces kinesin-5 motor domain with tubulin dimer. (a) Zoom in of panel (c). (b) Salt bridges at the interface of kinesin-5 motor domain and alpha tubulin. (c) Kinesin-5 motor domain at its binding position with tubulin dimer. Kinesin-5 motor domain is in red. Alpha and beta tubulins are shown in green and blue, respectively.

1.4 CONCLUSIONS

The main task of the kinesin-5 molecular motors is to crosslink the spindle microtubules and slide them to the spindle poles during the mitotic cell division of the cell. During the process, the kinesin-5 motor domains walk through the microtubules by hand over hand mechanism. While a motor domain is taking a step its courter part needs strong binding to microtubule, so that the motor domain can take a correct step to the future binding position. In this study we observed that the kinesin-5 motor domain has strong attractive interaction with the tubulin dimer as the binding interfaces of kinesin-5 motor domain and tubulins dimers are found to be oppositely charged. Furthermore, with binding energy calculations and salt bridges analysis, it is observed that the

interaction of kinsen-5 motor domain has strong interaction with beta tubulin. We do not have the direct evidence but while detaching from microtubule, kinesin-5 motor may first unbind with alpha tubulin because it has weaker interaction with alpha tubulin relative to its interaction with beta tubulin. The interfacial residues involved in salt bridges at both the interface s of kinesin-5 motor domain interacting with tubulin dimers, are the key residues. Which are believed to be the major drug targets. By means of which the process of sliding of spindle microtubules toward the spindle poles can be inhibited so that the proliferation of cancerous cell can be halted.

References

1. Wojcik, E.J., et al., *Kinesin-5: cross-bridging mechanism to targeted clinical therapy.* Gene, 2013. **531**(2): p. 133-149.
2. Kapitein, L.C., et al., *The bipolar mitotic kinesin Eg5 moves on both microtubules that it crosslinks.* Nature, 2005. **435**(7038): p. 114-118.
3. Kashina, A., G.C. Rogers, and J. Scholey, *The bimC family of kinesins: essential bipolar mitotic motors driving centrosome separation.* Biochimica et Biophysica Acta (BBA)-Molecular Cell Research, 1997. **1357**(3): p. 257-271.
4. Acar, S., et al., *The bipolar assembly domain of the mitotic motor kinesin-5.* Nature communications, 2013. **4**(1): p. 1-11.
5. Kashina, A., et al., *An essential bipolar mitotic motor.* Nature, 1996. **384**(6606): p. 225.
6. Scholey, J.E., et al., *Structural basis for the assembly of the mitotic motor Kinesin-5 into bipolar tetramers.* Elife, 2014. **3**: p. e02217.
7. Singh, S.K., et al., *Bidirectional motility of kinesin-5 motor proteins: structural determinants, cumulative functions and physiological roles.* Cellular and Molecular Life Sciences, 2018. **75**(10): p. 1757-1771.
8. Bannigan, A., et al., *A conserved role for kinesin-5 in plant mitosis.* Journal of cell science, 2007. **120**(16): p. 2819-2827.
9. Hagan, I. and M. Yanagida, *Kinesin-related cut 7 protein associates with mitotic and meiotic spindles in fission yeast.* Nature, 1992. **356**(6364): p. 74-76.
10. Enos, A.P. and N.R. Morris, *Mutation of a gene that encodes a kinesin-like protein blocks nuclear division in A. nidulans.* Cell, 1990. **60**(6): p. 1019-1027.

11. Heck, M., et al., *The kinesin-like protein KLP61F is essential for mitosis in Drosophila.* The Journal of cell biology, 1993. **123**(3): p. 665-679.

12. Mayer, T.U., et al., *Small molecule inhibitor of mitotic spindle bipolarity identified in a phenotype-based screen.* Science, 1999. **286**(5441): p. 971-974.

13. Sawin, K.E., T.J. Mitchison, and L.G. Wordeman, *Evidence for kinesin-related proteins in the mitotic apparatus using peptide antibodies.* Journal of Cell Science, 1992. **101**(2): p. 303-313.

14. von Loeffelholz, O., et al., *Cryo-EM structure (4.5-Å) of yeast kinesin-5–microtubule complex reveals a distinct binding footprint and mechanism of drug resistance.* Journal of molecular biology, 2019. **431**(4): p. 864-872.

15. Phillips, J.C., et al., *Scalable molecular dynamics on CPU and GPU architectures with NAMD.* The Journal of chemical physics, 2020. **153**(4): p. 044130.

16. Waterhouse, A., et al., *SWISS-MODEL: homology modelling of protein structures and complexes.* Nucleic acids research, 2018. **46**(W1): p. W296-W303.

17. Jorgensen, W.L., et al., *Comparison of simple potential functions for simulating liquid water.* The Journal of chemical physics, 1983. **79**(2): p. 926-935.

18. Humphrey, W., A. Dalke, and K. Schulten, *VMD: visual molecular dynamics.* Journal of molecular graphics, 1996. **14**(1): p. 33-38.

19. Darden, T., D. York, and L. Pedersen, *Particle mesh Ewald: An N· log (N) method for Ewald sums in large systems.* The Journal of chemical physics, 1993. **98**(12): p. 10089-10092.

20. Essmann, U., et al., *A smooth particle mesh Ewald method.* The Journal of chemical physics, 1995. **103**(19): p. 8577-8593.

21. Best, R.B., et al., *Optimization of the additive CHARMM all-atom protein force field targeting improved sampling of the backbone ϕ, ψ and side-chain $\chi1$ and $\chi2$ dihedral angles.* Journal of chemical theory and computation, 2012. **8**(9): p. 3257-3273.

22. Kollman, P.A., et al., *Calculating structures and free energies of complex molecules: combining molecular mechanics and continuum models.* Accounts of chemical research, 2000. **33**(12): p. 889-897.

23. Karki, C., et al., *A computational model of ESAT-6 complex in membrane.* Journal of Theoretical and Computational Chemistry, 2020. **19**(03): p. 2040002.

24. Xian, Y., et al., *The roles of electrostatic interactions in capsid assembly mechanisms of giant viruses.* International journal of molecular sciences, 2019. **20**(8): p. 1876.

25. Li, C., et al., *Highly efficient and exact method for parallelization of grid-based algorithms and its implementation in DelPhi.* Journal of computational chemistry, 2012. **33**(24): p. 1960-1966.

26. Li, L., et al., *DelPhi: a comprehensive suite for DelPhi software and associated resources.* BMC biophysics, 2012. **5**(1): p. 1-11.

27. Li, L., et al., *On the dielectric "constant" of proteins: smooth dielectric function for macromolecular modeling and its implementation in DelPhi.* Journal of chemical theory and computation, 2013. **9**(4): p. 2126-2136.

28. Dolinsky, T.J., et al., *PDB2PQR: expanding and upgrading automated preparation of biomolecular structures for molecular simulations.* Nucleic acids research, 2007. **35**(suppl_2): p. W522-W525.

Vita

My name is Chitra Bahadur Karki. I completed my undergraduate and graduate study form Tribhuvan University (TU), Nepal. I joined Liverpool International College as Physics lecture after my graduate studies and worked there for a year. In the fall of 2017, I joined The University of Texas at El Paso (UTEP) as a graduate student in Physics department. And later, on fall of 2019 I joined Computational Science Department. Here in UTEP, I joined Biophysics and Bioinformatics lab, Dr. Lin Li being research advisor. Under his supervision I was able to publish multiple papers and attain different conferences, where I was able to present research works via oral and poster presentations. I want to express my gratitude to Dr. Lin Li and all the members of Physics department for their valuable support and guidelines.